Electronic structure and magnetic properties of NaOsO_{3}

Yongping Du, Xiangang Wan, Li Sheng, Jinming Dong, and Sergey Y. Savrasov

Electronic structure and magnetic properties of NaOsO$_3$

Yongping Du,[1] Xiangang Wan,[1, 2, *] Li Sheng,[1] Jinming Dong,[1] and Sergey Y. Savrasov[2]

[1]*National Laboratory of Solid State Microstructures and Department of Physics, Nanjing University, Nanjing 210093, China*
[2]*Department of Physics, University of California, Davis, One Shields Avenue, Davis, CA 95616.*

(Dated: May 2, 2012)

A comprehensive investigation of the electronic and magnetic properties of NaOsO$_3$ has been made using the first principle calculations, in order to understand the importance of Coulomb interaction, spin–orbit coupling and magnetic order in its temperature–induced and magnetic–related metal–insulator transition. It is found that its electronic structure near the Fermi energy is dominated by strongly hybridized Os $5d$ and O $2p$ states. Despite of the large strength of spin–orbit coupling, it has only small effect on the electronic and magnetic properties of NaOsO$_3$. On the other hand, the on–site Coulomb repulsion affects the band structure significantly, but, a reasonable U alone cannot open a band gap. Its magnetism is itinerant, and the magnetic configuration plays an important role in determining the electronic structure. Its ground state is of a G–type antiferromagnet, and it is the combined effect of U and magnetic configuration that results in the insulating behavior of NaOsO$_3$.

I. INTRODUCTION

It is well known that the Coulomb interaction among $3d$ electrons in transition–metal oxides (TMO) is substantially important, which induces peculiar properties, such as metal–insulator transition[1], colossal magnetoresistance[2] and high critical temperature superconductivity[3]. Because the $5d$ orbitals are highly extended compared to those in the $3d$ systems, it is natural to expect that the electronic correlations are weak and have only negligible effect in the $5d$ compounds. However, recent theoretical and experimental works have given the evidence on the importance of Coulomb interactions here[4,5]. On the other hand, the spin–orbit coupling (SOC) in the $5d$ transition metal elements is expected to be strong due to the large atomic number[6]. Hence, due to the interplay of electron correlations and strong spin–orbit interactions, various anomalous electronic properties have been observed/proposed in the $5d$ transition oxides, such as J$_{eff}$=1/2 Mott state[4,5], giant magnetoelectric effect[7], high T$_c$ superconductivity[8], Weyl semimetal with Fermi arcs[9], Axion insulator with large magneto-electric coupling[10], topological insulator[11,12], correlated metal[13], Kitaev mode[14], etc.

One class of the well studied $5d$ compounds are the osmates[15–25]. For example, the physical properties of Cd$_2$Os$_2$O$_7$ are quite intriguing. It has been found that Cd$_2$Os$_2$O$_7$ is metallic at room temperatures, while undergoing a metal–insulator transition (MIT) at about 230 K[15]. Experiments reveal that this MIT is continuous and purely electronic. Moreover, it is coincident with a magnetic transition of antiferromagnetic (AFM) character[15,16]. Therefore, experimentalists argue that Cd$_2$Os$_2$O$_7$ is the first well–documented example of a pure Slater transition[16,26]. However, despite of the vast efforts devoted[15–20], its exact magnetic ground state configuration is still unknown due to the strong geometric frustration of the pyrochlore lattice. Therefore, theoretical evidence of the Slater transition in this compound is still lacking.

Recently, using high pressure technique, Shi *et al.*[21] synthesized another osmate: NaOsO$_3$. Similar to Cd$_2$Os$_2$O$_7$, NaOsO$_3$ also exhibits a temperature–induced MIT, which is again accompanied by a magnetic ordering without any lattice distortion[21]. However, better than Cd$_2$Os$_2$O$_7$, NaOsO$_3$ has a simple perovskite structure, consequently being free from the complication induced by magnetic frustration. Therefore, NaOsO$_3$ provides a unique platform to understand the temperature–induced and magnetic–related MIT. Based on the experimental crystal structure, Shi *et al.*[21] also perform the band-structure calculation for this compound. They[21] find that both LDA and LDA+SO calculation give the para-magnetic solution. Their numerical results[21] show that Coulomb U is not efficient, and antiferromagnetic corre-lation is essential to open the band gap[21]. Recently, there are experimental and theoretical evidences of the impor-tance of electronic correlation and spin-orbital coupling in 5d transition-metal compounds. Therefore a compre-hensive investigation of the effect of the Coulomb interac-tion, SOC and magnetic order on its electronic structure and MIT is still an interesting problem which we address in the present work.

II. METHOD

The electronic band structure calculations have been carried out by using the full potential linearized aug-mented plane wave method as implemented in WIEN2K package[27]. Local spin density approximation (LSDA) is widely used for various $4d$ and $5d$ transition metal oxides[4,5,25,28,29], and we therefore adopt it as the exchange–correlation potential. The muffin–tin radii for Na, Os and O are set to 1.13, 1.02, and 0.90 Å, respec-tively. The basic functions are expanded to R$_{mt}$K$_{max}$=7

(where R_{mt} is the smallest of the muffin-tin sphere radii and K_{max} is the largest reciprocal lattice vector used in the plane wave expansion), corresponding to 1915 LAPW functions at the Γ point. Using the second–order variational procedure[30], we include the spin–orbital coupling interaction (SOC), which has been found to play an important role in the $5d$ system[4,5,9,10]. A $10\times6\times10$ mesh is used for the Brillouin zone integral. The self–consistent calculations are considered to be converged when the difference in the total energy of the crystal does not exceed 0.1 mRy and that in the total electronic charge does not exceed 10^{-3} electronic charge at consecutive steps.

TABLE I: Numerical and experimental internal coordinates of $NaOsO_3$.

	calculation			experiment		
atom	x	y	z	x	y	z
Na	0.0392	1/4	0.9910	0.0328	1/4	-0.0065
O1	0.4919	1/4	0.0885	0.4834	1/4	0.0808
O2	0.2940	0.0428	0.7046	0.2881	0.0394	0.7112

$NaOsO_3$ has an orthorhombic perovskite structure with space group of $Pnma$[21]. There are four formula units (f.u.) per unit cell, and the 20 atoms in the unit cell can be classified as four nonequivalent crystallographic sites: Na, Os, O1 and O2 according to the symmetry. They are located at $4c$, $4b$, $4c$ and $8d$ sites, respectively and result in seven internal coordinates. From the X–ray diffraction experiment[21], the lattice constants of $NaOsO_3$ are determined to be $a=5.384$ Å, $b=7.580$ Å and $c=5.328$ Å, respectively. Based on the experimental lattice parameters, we optimize all independent internal atomic coordinates until the corresponding forces are less than 1 mRy/a.u. We confirm that the Coulomb U and SOC have only small effect on the crystal structure and list in Table I the internal atomic coordinates by LDA calculations. Our numerical internal coordinates are in good agreement with the experimental result, as shown in Table 1.

III. RESULTS AND DISCUSSIONS

Using the experimental lattice constants and the numerical internal coordinates, we first perform non–magnetic LDA calculation. The total density of states (TDOS), Os $5d$ partial density of states (PDOS), O1 $2p$ PDOS, O2 $2p$ PDOS, Na $2s$, $2p$ PDOS has been plotted in Fig.1(a)-(e), respectively. Our TDOS is very similar to that obtained based on the experimental crystal structure (See Fig.4a of Ref.[21]). The energy range, -9.0 to -2.4 eV is dominated by O1 $2p$ and O2 $2p$ bands with a small contribution from Os $5d$ state. Both Na $2s$ and $2p$ states, appearing mainly above 4 eV, have also considerable distribution between -9.0 to -2.4 eV, where O $2p$ state is mainly located, indicating the non–negligible hybridization between Na and O states despite that Na is highly
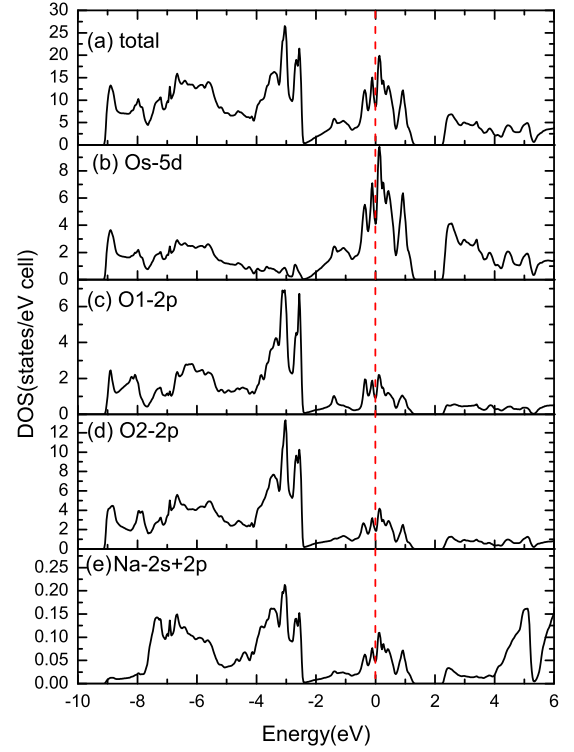

FIG. 1: Electronic density of states (DOS) from LDA calculation. Fermi energy E_f is set to zero. (a) TDOS, (b) Os $5d$ PDOS, (c) O1 $2p$ PDOS, (d) O2 $2p$ PDOS, (e) Na PDOS.
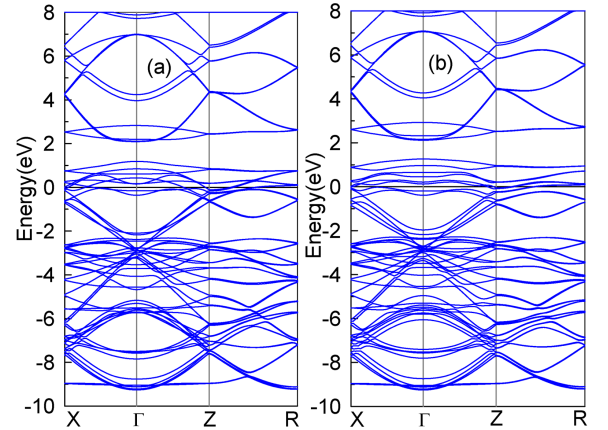

FIG. 2: Band structure of $NaOsO_3$, shown along the high symmetry directions. (a) LDA, (b) LDA+SO.

ionic. The Os atom is octahedrally coordinated by six O atoms, making the Os $5d$ band to split into the t_{2g} and e_g states, and the 12 t_{2g} bands are located from -2.8 to 1.2 eV, as shown in Fig. 2a. Due to the extended nature of $5d$ states, the crystal splitting between t_{2g} and e_g states is large, and the e_g states are located about 2.0 eV higher than the Fermi energy (E_f) and disperse widely. While providing the basic features of the electronic structure, LDA produces a metallic state due to partially occupied Os $5d$ t_{2g} band.
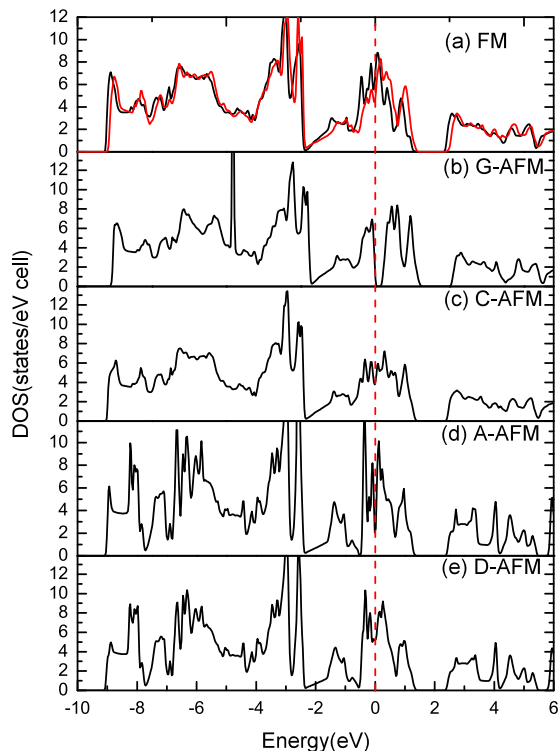
FIG. 3: Electronic density of states (DOS) from LDA+SO+U (U=2.0 eV) calculation. Fermi energy E_f is set to zero. (a) FM configuration, (b) G-AFM (c) C-AFM, (d) A-AFM (e) D-AFM. The black/red line is for up/down-spin, respectively. For AFM configurations, spin–up is the same as spin–down, thus only one spin channel is plotted.

TABLE II: Spin $\langle S \rangle$ and orbital $\langle O \rangle$ moment (in μ_B) as well as the total energy E_{tot} per unit cell (in eV) for several magnetic configurations, as calculated using LDA+U+SO method with U=2.0 eV. (E_{tot} is defined relative to the G–AFM configuration.).

Configuration	G–AFM	FM	C–AFM	A–AFM	D–AFM
E_{tot}	0	0.243	0.186	0.282	0.205
$\langle S \rangle$	0.94	0.22	0.54	0.29	0.20
$\langle O \rangle$	-0.11	-0.01	-0.04	-0.03	-0.03

been found that the electronic correlations are important for $5d$ TMO[4,5]. Moreover, the experiment reveal that $NaOsO_3$ has a long-range magnetic order at low temperature[21]. We therefore utilize LSDA+U scheme[31], which is adequate for searching for magnetically ordered insulating ground states[32]. Although, the accurate value of U is not known for perovskite osmates, the estimates of the values of U have been recently obtained between 1.4 and 2.4 eV in layered Sr_2IrO_4/Ba_2IrO_4[33]. We generally expect the screening to be larger in three dimensional (3D) systems than in two dimensional (2D) ones, and one can image that U in $NaOsO_3$ should be smaller than that in Sr_2IrO_4/Ba_2IrO_4. We therefore perform LDA+U+SO calculation and vary parameter U between 0.5 and 2.0 eV. Numerical results show that the electronic correlations can stabilize the FM configuration and narrow the Os t_{2g} band. However, as shown in Fig.3(a), our LDA+U+SO calculation with $U=$ 2.0 eV still gives a metallic solution. Naively, one may expect that using larger Coulomb U will result in an insulating state. However, consistent with Shi et al.[21], our additional calculations show that increasing U cannot solve this problem, and even a quite large U (=6.0 eV) cannot open the band gap. Therefore, electronic correlations alone cannot explain the insulating behavior, and the MIT is not of a Mott–type.

After studying the effect of SOC and U, we subsequently investigate the effect of various magnetic orders. We considered four antiferromagnetic (AFM) configurations besides the FM state: A–type AFM state (A–AFM) with layers of Os ions coupled ferromagnetically in a given set of (001) planes but with alternate planes having opposite spin orientation; C–type AFM state (C–AFM) with lines of Os ions coupled ferromagnetically in a given direction (001) but with alternate lines having opposite spin orientation; G–type AFM state (G–AFM) with Os ions coupled antiferromagnetically with all of their nearest neighbors; D–type AFM state (D–AFM) where Os ions lying within alternating planes perpendicular to [001] direction are coupled ferromagnetically along either [010] or [100] directions while different lines are coupled antiferromagnetically. Same as with the FM setup, the LSDA+SO calculation with $U=0$ for all considered AFM setups converges to the nonmagnetic metallic state.

On the other hand, the non–zero Coulomb interaction U of Os $5d$ is found to stabilize the AFM configura-

SOC of $5d$ electrons is about 0.5 eV[6], which is one order of magnitude larger than that of $3d$ electrons. Therefore, SOC usually changes the $5d$ band dispersion significantly and plays an essential role in the gap opening of Sr_2IrO_4 as well as of pyrochlore iridates[4,5,9]. In order to investigate the effect of SOC on the electronic structure, we compare the results obtained in the presence and absence of SOC, which are given in Fig. 2. The difference between the bands with and without SOC is small, as demonstrated in Fig.2. For $5d^5$ electronic configuration of Sr_2IrO_4[4], and $A_2Ir_2O_7$ (A=Y or rare earth)[9], where $J_{eff} = 1/2$ picture is valid, SOC has a dramatic effect on the band structure. In $NaOsO_3$, Os occurs in its 5^+ valence and there are 3 electrons in its t_{2g} band. Since t_{2g} band is half filled, it is natural to expect the effect of SOC to be small. As shown in Fig. 1a, the Fermi level is located near a sharp peak in the DOS. The relatively high density of states at the Fermi energy ($N(E_f)$) suggests the possibility of a Stoner instability against ferromagnetism (FM). Therefore, we perform a spin polarized calculation, however our LSDA+SO calculation with initial FM setup converges to the non–magnetic state. Thus consistent with Shi et al.[21], the FM state is not stable in LSDA+SO calculation.

Although the $5d$ orbitals are spatially extended, it has

tion. Our calculation confirms that the magnetic order has a significant effect, and for a reasonable U (≤ 2.0 eV), G–AFM configuration is the only insulating solution as shown in Fig.3. Moreover, regardless the value of U, the G–AFM configuration always has the lowest total energy. Thus we believe G–AFM configuration is the magnetic ordering state observed by the experiment[21] . With increasing U the band structure will change, but only when U is larger than 1.0 eV, the G–AFM solution becomes insulating. The DOS from U=1.0 eV (see the Fig.4c of Ref.21) is similar with that from U=2.0 eV (see Fig.3b of present work), which again indicates that the Coulomb U is not efficient to open the band gap. It is found that the magnetic moment is mainly located at Os site, and despite of strong hybridization between Os $5d$ and O $2p$, O site is basically non–magnetic (less than 0.003 μ_B). The numerical data for U=2.0 eV are given in Table II. For the $5d^5$ electronic systems such as $BaIrO_3$, Sr_2IrO_4, pyrochlore iridates etc, it has been found that due to the strong spin–orbit entanglement in $5d$ states, the magnetic orbital moment is about twice larger than the spin moment[4,5,9,34], even in the presence of strong crystal field and band effects. Contrary to $5d^5$ systems, the obtained orbital moment for $NaOsO_3$ is much smaller than its spin moment, showing again that SOC effect is small for this $5d^3$ electronic configuration case. As shown in Table II, the magnitude of magnetic moment is sensitive to the magnetic configuration, indicating the itinerant nature of magnetism. For the same U value, the G–AFM configuration always has the largest magnetic moment among the considered states. However, as shown in Table II, our numerical magnetic moment (0.83 μ_B) is much smaller than the experimental one[21]. For an itinerant magnet, one may still fit the $\chi(T)$ curve by the Curie–Weiss law, but cannot estimate the magnetic moment accurately based on the Curie–Weiss constant[35]. Thus, the experimental magnetic moment may not be reliable. The energy difference between various magnetic configurations is large, which is consistent with the observed high magnetic transition temperature (about 410 K)[21] although here one cannot estimate the interatomic exchange interaction and T_N based on the difference between total energies accurately as in the local moment systems[36]. Since the G–AFM configuration is the only insulating state, it is easy to understand that both magnetic and electronic phase transitions occur at the same temperature and our calculation indeed confirms that the MIT of $NaOsO_3$ is a Slater–type transition.

IV.   SUMMARY

In summary, we have investigated the detailed electronic structure and magnetic properties of $NaOsO_3$ using full potential linearized augmented plane wave method. Our results show that the electronic structure near the Fermi energy E_f is dominated by strongly hybridized Os $5d$ and O $2p$ states. Despite of its big value

the SOC has only weak effect on the band structure and magnetic moment. The electronic correlations alone cannot open the band gap, and the low temperature phase of $NaOsO_3$ is not a Mott–type insulator. The magnetic configuration has an important effect on the conductivity, and the ground state is a G–type AFM insulator. It is the interplay of the Coulomb interaction and magnetic ordering that result in the insulating behavior of $NaOsO_3$.

* Corresponding author: xgwan@nju.edu.cn

[1] M. Imada, A. Fujimori, and Y. Tokura, Rev. Mod. Phys. **70**, 1039 (1998).

[2] S. Jin, T. H. Tiefel, M. McCormack, R. A. Fastnacht, R. Ramesh and L. H. Chen, Science **264**, 413 (1994); P. Schiffer, A. P. Ramirez, W. Bao, and S-W. Cheong, Phys. Rev. Lett. **75**, 3336 (1995).

[3] W. Pickett, Rev. Mod. Phys. **61**, 433 (1989).

[4] B.J. Kim, Hosub Jin, S. J. Moon, J.-Y. Kim, B.-G. Park, C. S. Leem, Jaejun Yu, T. W. Noh, C. Kim, S.-J. Oh, J.-H. Park, V. Durairaj, G. Cao, and E. Rotenberg, Phys. Rev. Lett. **101**, 076402 (2008); B.J. Kim, H. Ohsumi, T. Komesu, S. Sakai, T. Morita, H. Takagi, and T. Arima, Science **323**, 1329 (2009).

[5] H. Jin, H. Jeong, T. Ozaki and J. Yu, Phys. Rev. B **80**, 075112 (2009).

[6] L.F. Mattheiss, Phys. Rev. B **13**, 2433 (1976).

[7] S. Chikara, O. Korneta, W. P. Crummett, L. E. DeLong, P. Schlottmann and G. Cao, Phys. Rev. B **80**, 140407 (R) (2009).

[8] F. Wang and T. Senthil, Phys. Rev. Lett. **106**, 136402 (2011).

[9] X. Wan, A.M. Turner, A. Vishwanath, and S.Y. Savrasov, Phys. Rev. B **83**, 205101 (2011).

[10] X. Wan, A. Vishwanath, and S. Y. Savrasov, Phys. Rev. Lett **108**, 146601 (2012).

[11] D.A. Pesin and L. Balents, Nature Physics **6**, 376 (2010).

[12] H.-M. Guo and M. Franz, Phys. Rev. Lett **103**, 206805 (2009). B. J. Yang, Y. B. Kim, Phys. Rev. B **82**, 085111 (2010). M. Kargarian, J. Wen, G. A. Fiete, Phys. Rev. B **83**, 165112 (2011).

[13] T. F. Qi, O. B. Korneta, X. Wan, G. Cao, arXiv:1201.0538 (2012).

[14] G. Jackeli and G. Khaliulin, Phys. Rev. Lett. **102**, 017205 (2009).

[15] W. Sleight, J. L. Gillson, J. F. Weiher, and W. Bindloss, Solid State Commun. **14**, 357 (1974).

[16] D. Mandrus, J.R. Thompson, R. Gaal, L. Forro, J.C. Bryan, B.C. Chakoumakos, L.M. Woods, B.C. Sales, R.S. Fishman, and V. Keppens, Phys. Rev. B **63**, 195104 (2001); W. J. Padilla, D. Mandrus and D. N. Basov, Phys. Rev. B **66**, 035120 (2002).

[17] Y. H. Matsuda, J. L. Her, S. Michimura, T. Inami, M. Suzuki, N. Kawamura, M. Mizumaki, K. Kindo, J. Yamauara, and Z. Hiroi, Phys. Rev. B **84**, 174431 (2011).

[18] A. Koda, R. Kadono, K. Ohishi, S. R. Saha, W. Higemoto, S. Yonezawa, Y. Muraoka, Z. Hiroi, J. Phys. Soc. Japan **76**, 063703 (2007).

[19] D. J. Singh, P. Blaha, K. Schwarz and J. O. Sofo, Phys. Rev. B **65**, 155109 (2002); H. Harima, J. Phys. Chem. Solids **63**, 1035 (2002).

[20] H. Shinaoka, T. Miyake, S. Ishibashi, arXiv:1111.6347 (2011).

[21] Y.G. Shi, Y.F. Guo, S. Yu, M. Arai, A.A. Belik, A. Sato, K. Yamaura, E. Takayama-Muromachi, H.F. Tian, H.X. Yang, J.Q. Li, T. Varga, J.F. Mitchell, and S. Okamoto, Phys. Rev. B **80**, 161104 (2009).

[22] A. S. Erickson, S. Misra, G. J. Miller, R. R. Gupta, Z. Schlesinger, W. A. Harrison, J. M. Kim, and I. R. Fisher, Phys. Rev. Lett. **99**, 016404 (2007).

[23] K.-W. Lee, W. E. Pickett, EPL **80**, 37008 (2007).

[24] Z. Hiroi, S. Yonezawa, Y. Muraoka, J. Phys. Soc. Jpn. **73**, 1651 (2004); , R. Saniz, J. E. Medvedeva, L.-H. Ye, T. Shishidou, and A. J. Freeman, Phys. Rev. B **70**, 100505 (2004).

[25] J. Kuneš, T. Jeong and W.E. Pickett, Phys. Rev. B **70**, 174510 (2004).

[26] J. C. Slater, Phys. Rev. **82**, 538 (1951).

[27] P. Blaha, K. Schwarz, G. K. H. Madsen, D. Kvasnicka, and J. Luitz, WIEN2k, An Augmented Plane Wave + Local Orbitals Program for Calculating Crystal Properties (Karlheinz Schwarz, Technische Universität Wien, Austria), 2001, ISBN3–9501031–1–2.

[28] K. Maiti, Solid State Commun. **149**, 1351 (2009); K. Maiti, Phys. Rev. B **73**, 115119 (2006).

[29] D. J. Singh, J. Appl. Phys. **79**, 4818 (1996); A. T. Zayak, X. Huang, J. B. Neaton, and K. M. Rabe, Phys. Rev. B **77**, 214410 (2008); X. Wan, J. Zhou, and J. Dong, Europhys. Lett. **92**, 57007 (2010).

[30] D.D. Koelling, B.N. Harmon, J. Phys. C **10**, 3107 (1977).

[31] V.I. Anisimov, F. Aryasetiawan, and A.I. Lichtenstein, J. Phys.: Condens. Matter **9**, 767 (1997).

[32] G. Kotliar, S. Y. Savrasov, K. Haule and V. S. Oudovenko, Rev. Mod. Phys. **78**, 865 (2006).

[33] R. Arita, J. Kuneš, A.V. Kozhevnikov, A.G. Eguiluz, M. Imada, arXiv:1107.0835 (2011).

[34] M. A. Laguna-Marco1, D. Haskel, N. Souza-Neto, J. C. Lang, V. V. Krishnamurthy, S. Chikara, G. Cao, and M. van Veenendaal, Phys. Rev. Lett. **105**, 216407 (2010).

[35] T. Moriya, *Spin fluctuations in itinerant electron magnetism*, (Springer-Verlag, 1985).

[36] X. Wan, M. Kohno and X. Hu, Phys. Rev. Lett. **94**, 087205 (2005).